Optics Letters

Topological surface plasmons in superlattices with changing sign of the average permittivity

HANYING DENG,[1] XIANFENG CHEN,[1] NICOLAE C. PANOIU,[2] AND FANGWEI YE[1,*]

[1]Department of Physics and Astronomy, Shanghai Jiao Tong University, 800 Dongchuan Road, Shanghai 200240, China
[2]Department of Electronic and Electrical Engineering, University College London, Torrington Place, London WC1E7JE, UK
*Corresponding author: fangweiye@sjtu.edu.cn

Received 4 August 2016; revised 19 August 2016; accepted 19 August 2016; posted 22 August 2016 (Doc. ID 273114); published 12 September 2016

We address the topological properties of one-dimensional plasmonic superlattices composed of alternating metallic and dielectric layers. We reveal that the Zak phase of such plasmonic lattices is determined by the sign of the spatial average of their permittivity, $\bar{\epsilon}$, and as such the topology and their associated interfacial (edge) states are extremely robust against structural disorder. Our study shows that the topologically protected interfacial modes occurring at the interface between two plasmonic lattices with opposite signs of $\bar{\epsilon}$ can be viewed as the generalization of the conventional surface plasmon polaritons existing at metallic–dielectric interfaces.

OCIS codes: (350.4238) Nanophotonics and photonic crystals; (310.6628) Subwavelength structures, nanostructures; (240.6680) Surface plasmons; (240.6648) Surface dynamics.

http://dx.doi.org/10.1364/OL.41.004281

The nontrivial topological properties of matter have been attracting increasing interest in condensed matter physics, as the theory of band topology explains a series of striking phenomena like the quantum Hall effect [1–3] and topological insulators [4–8]. Starting from the duality between their mathematical description, similar concepts and ideas have been introduced into the realm of optics, and nontrivial topological effects have been demonstrated across a variety of optical systems [9]. Perhaps the simplest optically topological structure is analogous to the celebrated Su–Schrieffer–Heeger (SSH) model for polyacetylene [10], in which a chain of sites with alternating signs of the coupling constant exhibits two topologically distinct phases and topologically protected interfacial modes exist at the interface between two topologically distinct chains. Realization of the SSH model in photonic systems includes dimerized dielectric waveguides [11] and dielectric nanoparticles [12], as well as metallic nanodisks [13]. Furthermore, edge states between coupled plasmonic waveguides described by the SSH model have been investigated in graphene [14] and plasmonic waveguide arrays [15]. These structures are optically discrete, thus they closely mimic the original SSH model. On the other hand, topological properties and associated edge states of one-dimensional (1D) photonic structures have also been investigated in continuous periodic systems, i.e., beyond the tight-binding approximation and other discrete models [16,17].

All the topological properties of 1D structures mentioned above can be characterized by a single physical quantity, the so-called Zak phase [18]. This is a special kind of Berry phase, associated with 1D bulk bands. The characterization of the Zak phase of matter is of fundamental importance to the understanding of topology-related physical properties of condensed matter systems. Optics is emerging as an alternative platform to study such topology-induced phenomena, as in many cases it provides more suitable theoretical and experimental tools to explore them. In particular, specific ways to measure the Zak phase in optical systems have been proposed theoretically [19] and implemented experimentally by employing optical waveguide systems [20–23].

In this Letter, we focus on topological properties of 1D plasmonic superlattices composed of alternating metallic and dielectric layers. We reveal that the Zak phase of such superlattices is determined by the sign of the spatial average of the permittivity of the lattice, $\bar{\epsilon}$, such that lattices with $\bar{\epsilon} > 0$ are topologically distinct from those with $\bar{\epsilon} < 0$. Due to the fact that fully random structural perturbations of the superlattice that preserve the averaged values of the thickness of the constituent layers do not modify the value of $\bar{\epsilon}$ and consequently its sign, the topology and the associated interfacial (edge) states of the plasmonic superlattices are found to be extremely robust against such perturbations. Our analysis reveals that the topologically protected modes at the interface between two superlattices with opposite signs of the average permittivity represent a conceptual generalization of the well-known surface plasmon polaritons (SPPs) formed at metal/dielectric interfaces.

Let us consider a 1D plasmonic superlattice composed of alternating layers of metallic and dielectric materials stacked along the x-axis, as depicted in Fig. 1(a). To be more specific, we assume that the metallic and dielectric layers are made of silver and silicon, respectively. At the wavelength of $\lambda = 1550$ nm, the permittivity of dielectric (silicon) materials is $\epsilon_d = 12.25$ and the complex permittivity of the metal (silver) is $\epsilon_m = -125.39 + 2.84i$ [24]. Since the imaginary part of the permittivity of the metal is very small as compared to its real part, the influence of the metal loss (heat dissipation) on the

results are found to be negligible. Despite this, in the following analysis we have taken into account the small imaginary part of the permittivity of the metal, unless otherwise stated.

Considering the propagation along the z-axis of a TM-polarized optical beam (i.e., the only nonzero components of the electromagnetic fields are E_x, E_z, and H_y), one can readily find the photonic band structure of the superlattice by solving the following transcendental equation:

$$\cos(k_x\Lambda) = \cos(k_d t_d)\cos(k_m t_m) - \frac{1}{2}\left(\frac{\zeta_d}{\zeta_m} + \frac{\zeta_m}{\zeta_d}\right)\sin(k_d t_d)\sin(k_m t_m), \quad (1)$$

where k_x is the Bloch wavevector, k_z is the propagation wavevector, $k_j = \sqrt{(\omega/c)^2\epsilon_j\mu_j - k_z^2}$, $\zeta_j = k_j/\epsilon_j$, $(j = d,\ m)$, t_d and t_m are the thickness of dielectric and metallic layers, respectively, $\Lambda = t_d + t_m$ is the period of the superlattice, and c is the light speed in vacuum. By fixing the frequency ω in Eq. (1), the dependence $k_z = k_z(k_x)$ defines the photonic band structure (spatial dispersion relation) for that particular frequency [25]. The dependence of the band structure on the thickness of the metallic layer is shown in Fig. 1(b) for a fixed thickness of the dielectric layer, $t_d = 240$ nm. Note that choosing a specific value for t_d does not make our analysis less general. However, it should be mentioned that, in order for a two-band configuration to occur, as it is required in this study for reasons that will become apparent later, t_d should be larger than a certain critical value (for example, for $t_m = 25$ nm, the minimum t_d required is 199 nm).

A known property of the band structure of plasmonic superlattices is that when the spatially averaged permittivity of the superlattice is zero, namely, when $\bar{\epsilon} = \frac{\epsilon_d t_d + \epsilon_m t_m}{t_d + t_m} = 0$, a diabolical point (DP)—the 1D counterpart of Dirac points—appears at the center of Brillouin zone, $k_x = 0$ [25–27]. This property is illustrated in Figs. 1(b) and 1(c), as indeed for some specific value of t_m (in the example shown in these plots, $t_m = 23.45$ nm), the condition $\bar{\epsilon} = 0$ holds. Moreover, for this specific value of t_m, the upper band touches the lower one in such a way that a DP is formed at $(k_x, k_z) = (0, k_z^{\mathrm{DP}})$, where $k_z^{\mathrm{DP}} = k_0\sqrt{\epsilon_m\epsilon_d/(\epsilon_m + \epsilon_d)}$. On the other hand, once the zero-average-permittivity condition is broken, namely, when either $\bar{\epsilon} > 0$ or $\bar{\epsilon} < 0$, the DP vanishes and a gap opens. Upon understanding this mechanism of formation of a DP, an interesting question arises, i.e., in the context of light wave interactions with such superlattices what are the differences between a superlattice with $\bar{\epsilon} > 0$ and one with $\bar{\epsilon} < 0$?

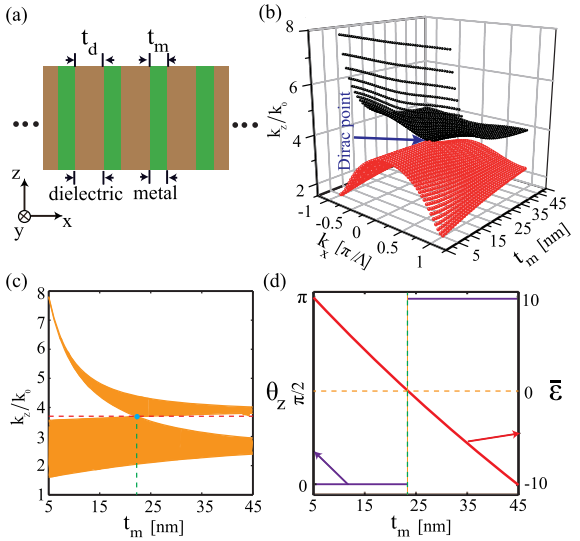

Fig. 1. (a) Schematic of a dielectric–metal layered lattice. (b) Dependence of photonic band structure $k_z(k_x)$ on the thickness of the metallic layer, t_m. A DP appears in the band structure at $t_m = 23.45$ nm, for which $\bar{\epsilon} = 0$. (c) Lattice transmission bands (orange domains) versus metallic layer thickness. (d) Zak phase and average permittivity $\bar{\epsilon}$ of the lattice versus t_m. In these calculations, $\lambda = 1550$ nm, $t_d = 240$ nm, $\epsilon_m = -125.39$, and $\epsilon_d = 12.25$.

To answer this question, we study the topological properties of these superlattices by calculating the Zak phase of their bulk bands, defined by the following formula [18]:

$$\theta_z = \int_{-\pi/\Lambda}^{\pi/\Lambda}\left(i\int_{\mathrm{unitcell}}\psi_{n,k_x}^{*}\frac{\partial\psi_{n,k_x}}{\partial k_x}\mathrm{d}x\right)\mathrm{d}k_x, \quad (2)$$

where ψ_{n,k_x} is the periodic-in-cell part of the Bloch magnetic field eigenfunction of a state belonging to the nth band at k_x, i.e., $H_{y,n,k_x}(x) = \psi_{n,k_x}(x)\exp(ik_x x)$. The function $\psi_{n,k_x}(x)$ can be obtained analytically using the transfer-matrix method [28]. The Zak phase depends on the choice of the origin, and here we choose this origin to be the center of the dielectric layer.

The outcome of the calculation of the Zak phase is shown in Fig. 1(d). As expected, the value of θ_z is binary valued, being equal to either 0 or π. Importantly, the Zak phase of the plasmonic superlattices is found to be solely dependent on the sign of the average permittivity, thus being independent of the particular geometry of the superlattice or the values of the permittivity of the layers. Specifically, it is equal to zero if $\bar{\epsilon} > 0$ and is equal to π when $\bar{\epsilon} < 0$. In other words, the topology of plasmonic superlattices is uniquely defined by the sign of $\bar{\epsilon}$, and structural transformations or geometrical fluctuations preserve the superlattice topology provided that $\bar{\epsilon}$ does not change its sign. If, on the other hand, the plasmonic superlattice is structurally transformed in such a way that $\bar{\epsilon}$ changes its sign after it passes through the zero point, as per Fig. 1(d), θ_z varies accordingly, leading to the modification of the topology of the superlattice. Note also that by changing the origin with respect to which the Zak phase is calculated the two constant values change. However, the same phase shift of π occurs when $\bar{\epsilon}$ changes its sign.

The dependence of the topology of plasmonic superlattices on the sign of $\bar{\epsilon}$ can be explained by the general topological band theory. As mentioned, a DP appears in the band structure of lattices when $\bar{\epsilon} = 0$ and it vanishes (with a gap opening in the band structure) when $\bar{\epsilon}$ becomes nonzero. Following the general topological band theory, which states that the topological phase of matter changes when a bandgap closes at a DP and then reopens when the system is further modified [4,5], we therefore expect that the topology of plasmonic superlattices is indeed characterized by the sign of $\bar{\epsilon}$ and remains invariant as long as the sign of $\bar{\epsilon}$ is preserved. Thus, a fundamental result of this analysis is that we can directly link in a simple way the topology of plasmonic superlattices to a single invariant parameter characterizing the plasmonic structure, namely, the sign of the average dielectric permittivity! This finding may have practical implications on the design and characterization of topologically functional devices implemented using plasmonic

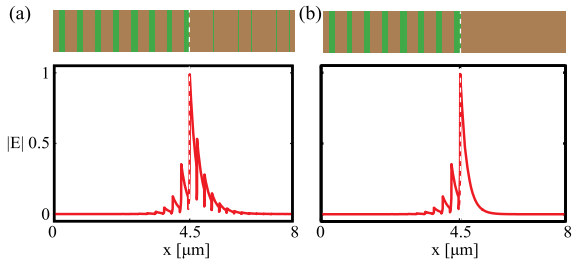

Fig. 2. (a) Profile of the electric field of the surface mode located at the interface between a plasmonic lattice with $t_m = 45$ nm ($\bar{\epsilon} = -9.48 + 0.45i$) and a plasmonic lattice with $t_m = 10$ nm ($\bar{\epsilon} = 6.74 + 0.11i$). (b) The same as in (a) but with the second superlattice replaced by a uniform dielectric medium with $\epsilon = 12.25$. The white dashed lines indicate the position of the interface. The remaining parameters are $t_d = 240$ nm, $\epsilon_m = -125.39 + 2.84i$, and $\epsilon_d = 12.25$.

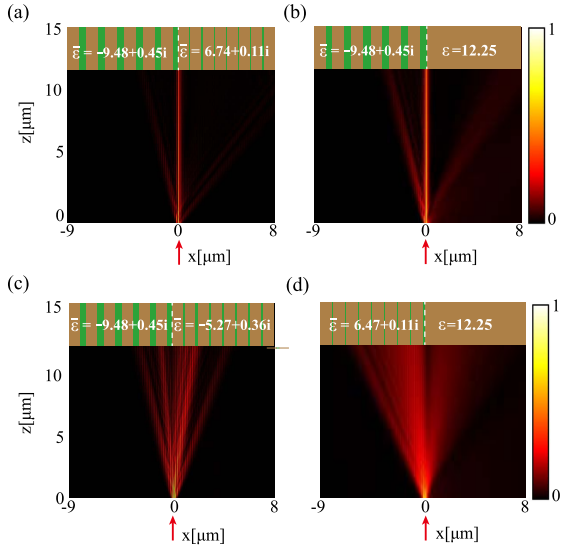

Fig. 3. Top (bottom) panels show the evolution of the normalized electric field amplitude when a TM-polarized Gaussian beam is injected normally at the interface between two plasmonic superlattices with opposite (the same) signs of $\bar{\epsilon}$. In the right panels, one of the superlattices is replaced by a homogeneous medium. The average of the dielectric permittivity for each superlattice and medium is indicated in the figure. The E_x component of the input Gaussian beam is given by $E_x(x) = \exp[-x^2/(3t_d)^2]$, whereas $t_d = 240$ nm is the thickness of the dielectric layers. Red arrows indicate the location of the incident beam.

nanostructures. Equally important is that these ideas can potentially be extended to other 1D superlattices characterized by spatially averaged rather than local physical quantities, such as zero-$\bar{n}$ superlattices [29–31]. Our findings also imply that, if for instance graphene sheets are incorporated in superlattices, electrically or optically tunable topological nanodevices can be achieved thanks to the tunability of graphene [27].

Consider now two adjacent, semi-infinite plasmonic superlattices, and let us investigate the possibility that localized states exist at the interface between superlattices. The two superlattices are designed to have different signs of $\bar{\epsilon}$ by, for example, using different thicknesses of the metallic layers, as illustrated in Fig. 2(a), or even setting $t_m = 0$ for one superlattice, which means that the superlattice becomes a pure dielectric medium [see Fig. 2(b)]. Consistent with the bulk-edge correspondence principle, which states that localized zero-energy states exist at the interface between two insulators with distinct band topology, our mode analysis of such interfacial systems reveals that if two connected superlattices differ in their sign of $\bar{\epsilon}$, localized modes always appear at the interface separating the two superlattices. On the other hand, if the sign of $\bar{\epsilon}$ for both superlattices is the same, their interface supports no localized modes. This is similar to the case of surface waves at the interface between two homogeneous and isotropic media, namely, such localized modes, called SPPs, exist only if the permittivities of the two media have opposite signs. Indeed, the field profile of the surface modes in Fig. 2 resembles that of SPPs, with the additional feature being the field oscillations in superlattices.

The above analysis is further corroborated by our direct beam propagation simulations. Specifically, we launched normally onto the interface a TM-polarized Gaussian beam of narrow width, $w \approx 3t_d$, and determined the electromagnetic field as it propagated into the superlattice. As expected, when the sign of $\bar{\epsilon}$ in the two adjacent superlattices takes different values, a localized mode quickly forms at the interface while the extra energy of the input wave diffracts as radiative waves [see Figs. 3(a) and 3(b)]. In contrast, when the sign of $\bar{\epsilon}$ of the two adjacent superlattices is the same [negative in Fig. 3(c) and positive in Fig. 3(d)], the input optical beam strongly diffracts without any signature of the formation of a surface mode being observed.

As the topology of plasmonic superlattices is determined by the sign of the averaged permittivity, one expects that the topology and the associated interfacial states are extremely robust against structural disorder. This is expected because a fully random perturbation of the structure that preserves the averaged values of the thickness of the constituent layers does not modify the spatially averaged dielectric permittivity or its sign. To test this conjecture, we consider two adjacent superlattices, as shown in Fig. 2, but now introduce disorder into them by defining a random fluctuation of the thickness of the metallic components. Thus, the thickness of the nth Ag layer in each plasmonic lattice is set to $t_m^n = t_{m0} + \delta_n$, where t_{m0} is the average thickness, and δ_n is a random value. We assume δ_n to be uniformly distributed in the interval of $[-\delta, \delta]$, $0 < \delta < t_{m0}$. Hence, the level of disorder can be characterized by the parameter $\Delta \equiv \delta/t_{m0}$. The spectra and field profile of the interface modes determined for increasing disorder strength, Δ, are shown in Fig. 4.

It is known that incorporating disorder in a 1D lattice always leads to the formation of localized Anderson modes. Anderson modes strongly depend on the disorder strength, with their degree of spatial localization increasing with the disorder strength, Δ. The eigenvalue spectra of Anderson modes were statistically averaged over 50 randomly perturbed superlattice configurations, with the results presented in Fig. 4(a). It shows that, as expected, the Bragg gap of the unperturbed lattices narrows as Δ increases [32]. In sharp contrast, the wave profile of the interfacial mode remains almost unchanged, even when the disorder strength increases to 80% and above, as shown in Figs. 4(b) and 4(c). Furthermore, the eigenvalue k_z

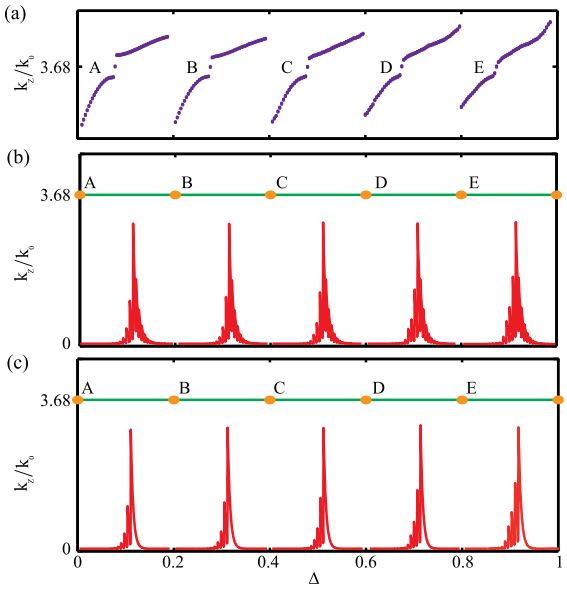

Fig. 4. (a) Spectrum of Anderson modes and (b),(c) dependence of eigenvalue (green line) and electric field amplitude (red curve) of the interfacial mode on the disorder level, calculated for the interface system composed of two plasmonic lattices that, in the unperturbed limit, are the same as those shown in Figs. 2(a) and 2(b), respectively. The mode profiles and the spectrum of the Anderson modes are calculated for five disorder levels: (A) 0%, (B) 20%, (C) 40%, (D) 60%, and (E) 80%. The dot inside the bandgap of Fig. 4(a) corresponds to the interface mode. All results are obtained by an ensemble average over 50 disorder realizations.

(propagation constant) of the interfacial mode is unaffected by structural disorder. The interfacial mode is actually pinned at the photonic DP of the unperturbed superlattice with $\bar{\epsilon} = 0$, namely, the eigenvalue of the interfacial mode is given by $k_z^{\mathrm{DP}} = k_0\sqrt{\varepsilon_m\varepsilon_d/(\varepsilon_m + \varepsilon_d)}$. Note that this eigenvalue is equal to that of conventional SPPs formed at the interface between a semi-infinite metal and a semi-infinite dielectric medium [33]. Therefore, the topologically protected interface modes, localized at the interface between two superlattices characterized by different signs of $\bar{\epsilon}$, represent a natural generalization of the conventional SPPs. Compared to conventional SPPs, however, such generalized SPP waves obviously have more degrees of freedom, which makes them an appealing alternative to be employed in nanophotonic applications. For example, by properly choosing the parameters of the two superlattices, it could be possible to engineer and reduce the losses of topological SPPs below those of conventional SPPs.

In summary, we have studied the topological properties of plasmonic superlattices and revealed that their topology is determined by the sign of their spatially averaged dielectric permittivity. As such, their topology and the associated edge (interface) states are extremely robust against the structural random perturbations. Such topologically protected localized states at the interface between two superlattices with opposite signs of the average permittivity represent a natural generalization of the well-known SPPs supported by metal/dielectric interfaces.

Funding. National Natural Science Foundation of China (NSFC) (61475101); Innovation Program of Shanghai Municipal Education Commission (13ZZ022); Doctoral Program Foundation of Institutions of Higher Education of China (20110073120074); European Research Council (ERC) (ERC-2014-CoG-648328)

REFERENCES

1. D. Thouless, M. Kohmoto, M. Nightingale, and M. Den Nijs, Phys. Rev. Lett. **49**, 405 (1982).
2. C. L. Kane and E. J. Mele, Phys. Rev. Lett. **95**, 146802 (2005).
3. B. A. Bernevig, T. L. Hughes, and S.-C. Zhang, Science **314**, 1757 (2006).
4. M. Z. Hasan and C. L. Kane, Rev. Mod. Phys. **82**, 3045 (2010).
5. X.-L. Qi and S.-C. Zhang, Rev. Mod. Phys. **83**, 1057 (2011).
6. L. H. Wu and X. Hu, Phys. Rev. Lett. **114**, 223901 (2015).
7. H. Wang, L. Xu, H. Chen, and J. Jiang, Phys. Rev. B **93**, 235155 (2016).
8. L. Xu, H. Wang, Y. Xu, H. Chem, and J. Jiang, Opt. Express **24**, 18059 (2016).
9. L. Lu, J. D. Joannopoulos, and M. Soljacic, Nat. Photonics **8**, 821 (2014).
10. W. Su, J. R. Schrieffer, and A. J. Heeger, Phys. Rev. Lett. **42**, 1698 (1979).
11. H. Schomerus, Opt. Lett. **38**, 1912 (2013).
12. A. P. Slobozhanyuk, A. N. Poddubny, A. E. Miroshnichenko, P. A. Belov, and Y. S. Kivshar, Phys. Rev. Lett. **114**, 123901 (2015).
13. I. S. Sinev, I. S. Mukhin, A. P. Slobozhanyuk, A. N. Poddubny, A. E. Miroshnichenko, A. K. Samusev, and Y. S. Kivshar, Nanoscale **7**, 11904 (2015).
14. L. Ge, L. Wang, M. Xiao, W. Wen, C. T. Chan, and D. Han, Opt. Express **23**, 21585 (2015).
15. Q. Cheng, Y. Pan, Q. Wang, T. Li, and S. Zhu, Laser Photon. Rev. **9**, 392 (2015).
16. N. Malkova, I. Hromada, X. Wang, G. Bryant, and Z. Chen, Opt. Lett. **34**, 1633 (2009).
17. M. Xiao, Z. Q. Zhang, and C. T. Chan, Phys. Rev. X **4**, 021017 (2014).
18. J. Zak, Phys. Rev. Lett. **62**, 2747 (1989).
19. S. Longhi, Opt. Lett. **38**, 3716 (2013).
20. M. Atala, M. Aidelsburger, J. T. Barreiro, D. Abanin, T. Kitagawa, E. Demler, and I. Bloch, Nat. Phys. **9**, 795 (2013).
21. A. Blanco-Redondo, I. Andonegui, M. J. Collins, G. Harari, Y. Lumer, M. C. Rechtsman, B. J. Eggleton, and M. Segev, Phys. Rev. Lett. **116**, 163901 (2016).
22. W. S. Gao, M. Xiao, C. T. Chan, and W. T. Tam, Opt. Lett. **40**, 5259 (2015).
23. Q. Wang, M. Xiao, H. Liu, S. Zhu, and C. T. Chan, Phys. Rev. B **93**, 041415 (2016).
24. P. B. Johnson and R.-W. Christy, Phys. Rev. B **6**, 4370 (1972).
25. S. H. Nam, A. J. Taylor, and A. Efimov, Opt. Express **18**, 10120 (2010).
26. L. Sun, J. Gao, and X. Yang, Opt. Express **21**, 021542 (2013).
27. H. Deng, F. Ye, B. A. Malomed, X. Chen, and N. C. Panoiu, Phys. Rev. B **91**, 201402 (2015).
28. P. Yeh, A. Yariv, and C.-S. Hong, J. Opt. Soc. Am. **67**, 423 (1977).
29. J. Li, L. Zhou, C. T. Chan, and P. Sheng, Phys. Rev. Lett. **90**, 083901 (2003).
30. N. C. Panoiu, R. M. Osgood, S. Zhang, and S. R. J. Brueck, J. Opt. Soc. Am. B **23**, 506 (2006).
31. S. Kocaman, R. Chatterjee, N. C. Panoiu, J. F. McMillan, M. B. Yu, R. M. Osgood, D. L. Kwong, and C. W. Wong, Phys. Rev. Lett. **102**, 203905 (2009).
32. H. Deng, X. Chen, B. A. Malomed, N. C. Panoiu, and F. Ye, Sci. Rep. **5**, 15585 (2015).
33. S. Maier, *Plasmonics: Fundamentals and Applications* (Springer, 2007).